Model for the Magnetic Order and Pairing Channels in Fe Pnictide Superconductors

M. Daghofer,[1,2] A. Moreo,[1,2] J. A. Riera,[3] E. Arrigoni,[4] D. J. Scalapino,[5] and E. Dagotto[1,2]

[1]*Department of Physics and Astronomy, The University of Tennessee, Knoxville, Tennessee 37996, USA*
[2]*Materials Science and Technology Division, Oak Ridge National Laboratory, Oak Ridge, Tennessee 32831, USA*
[3]*Instituto de Física Rosario, Consejo Nacional de Investigaciones Científicas y Técnicas, Universidad Nacional de Rosario, 2000-Rosario, Argentina*
[4]*Institute of Theoretical and Computational Physics, TU Graz, A-8010 Graz, Austria*
[5]*Department of Physics, University of California, Santa Barbara, California 93106-9530, USA*

(Received 1 May 2008; published 4 December 2008)

A two-orbital model for Fe-pnictide superconductors is investigated using computational techniques on two-dimensional square clusters. The hopping amplitudes are derived from orbital overlap integrals, or by band structure fits, and the spin frustrating effect of the plaquette-diagonal Fe-Fe hopping is remarked. A spin striped state is stable in a broad range of couplings in the undoped regime, in agreement with neutron scattering. Adding two electrons to the undoped ground state of a small cluster, the dominant pairing operators are found. Depending on the parameters, two pairing operators were identified: they involve inter-xz-yz orbital combinations forming spin singlets or triplets, transforming according to the B_{2g} and A_{2g} representations of the D_{4h} group, respectively.

DOI: 10.1103/PhysRevLett.101.237004 PACS numbers: 74.20.Mn, 71.27.+a, 74.20.Rp, 74.70.−b

Introduction.—The recent discovery of superconductivity in the layered rare-earth oxypnictides compounds $LnO_{1-x}F_xFeAs$ (Ln = La, Pr, Ce, Sm) has captured the attention of the condensed matter community [1]. The high current record critical temperature $T_c \sim 55$ K in $SmO_{1-x}F_xFeAs$ [2] suggests that an unconventional pairing mechanism may be at work [3,4].

As for Cu-based high temperature superconductors (HTSC), the analysis of undoped compounds, such as LaOFeAs, is expected to provide important information toward the understanding of the superconducting state reached by ~10% F doping. Neutron scattering experiments have provided evidence of magnetic order in LaOFeAs at 134 K: Fe spins order into ferromagnetic ''stripes'' that are aligned antiferromagnetically [5–7]. In the two-dimensional (2D) square lattice notation, the LaOFeAs magnetic structure factor has peaks at wave vectors $q \sim (0, \pi)$, $(\pi, 0)$ [5–7]. Assuming a smooth continuity between the undoped and F-doped compounds, the pairing mechanism could be magnetic in origin and triggered by this unusual magnetic state.

Theoretical work on the new superconductors includes band structure calculations that have shown the relevance of the 3d levels of Fe [8,9]. A metallic state involving a Fermi surface (FS) made out of disconnected small pieces (''pockets'') was predicted [8]. To understand some of the properties of the undoped limit, electron correlations appear to be important [10]. Two-orbitals descriptions [11,12] and other models have been proposed, and a variety of approximations have led to several unconventional pairing channel proposals [13–15].

Our purpose is to report the first unbiased computational results obtained using a model Hamiltonian for Fe pnictides, with emphasis on a real-space description. In the undoped limit, a spin striped magnetic state is obtained and explained. With light electron doping, novel pairing operators are identified. The path followed here mimics research in the HTSC, where the computational study of model Hamiltonians in real-space [16] provided a perspective dual to momentum-space diagrammatic calculations. In fact, early numerical studies of the 2-hole state on small t-J clusters indicated that the pairing was in the $d_{x^2-y^2}$ channel [16]. Thus, it is natural to follow a similar path for the new Fe superconductors.

Model and techniques.—Fe pnictides have a layered structure, with the Fe atoms forming a 2D square lattice and the As atoms located above or below the plane, at the centers of alternating plaquettes; see Fig. 1(a). Here, the emphasis will be on the Fe d_{xz} and d_{yz} degenerate states [11,12] since band structure calculations have shown the importance of these orbitals at the Fermi surface [4,17]. Since the complexity of the problem rapidly increases with the number of orbitals, it is reasonable to start with just two orbitals, contrast the results with experiments, and slowly build up a more realistic model with extra orbitals. To estimate the hopping amplitudes, the Slater-Koster (SK) tight-binding scheme is followed [18]. This approach is simple, analytical, and leads to a geometrical understanding of the magnetic phase. The SK method for the hopping integrals needs as input the location of the Fe and As atoms, and the nature of the orbitals. The Fe-Fe (Fe-As) distance used is $r = 2.854$ Å ($s = 2.327$ Å). The effective Fe-Fe hopping amplitudes—via As—are the product of the direct Fe-As hoppings; the three p orbitals were taken into account on the intermediate As ion. Two Fe-As-Fe paths connect nearest-neighbor (NN) Fe sites, while only one

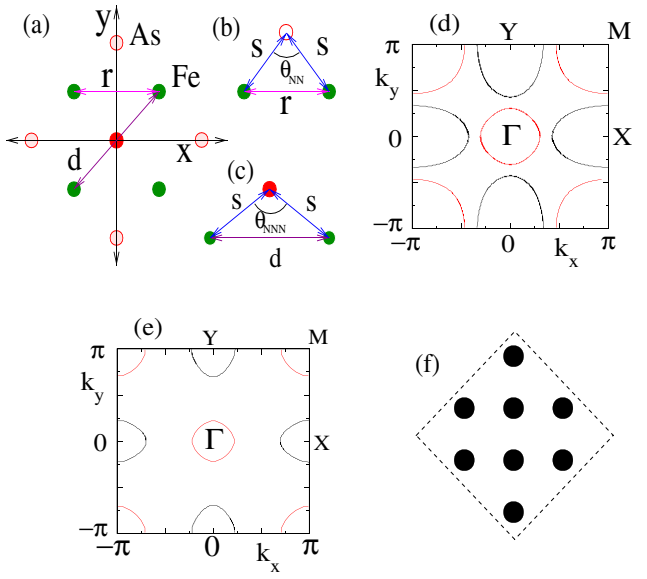

FIG. 1 (color online). (a) Geometry of the FeAs layer. As atoms are located above (open circles) or below (filled circle at the origin) the Fe plane (remaining filled circles). (b) The Fe-Fe NN path. (c) The Fe-Fe NNN path. (d) Fermi surface of H_{FeAs} for $pd\pi/pd\sigma = -0.2$ in the $U = J = 0$ limit. (e) Same as (d) but for the parameters of Ref. [11]. In (d), the half-filled chemical potential is at -0.03. (f) The tilted 8-site cluster used here.

exists for next-nearest-neighbor (NNN) Fe's along the plaquette diagonals. The kinetic energy of the resulting model restricted to Fe sites is

$$\begin{aligned} H_k = & -t_1 \sum_{\mathbf{i},\sigma} (d^\dagger_{\mathbf{i},x,\sigma} d_{\mathbf{i}+\hat{x},x,\sigma} + d^\dagger_{\mathbf{i},y,\sigma} d_{\mathbf{i}+\hat{y},y,\sigma} + \mathrm{H.c.}) \\ & - t_2 \sum_{\mathbf{i},\sigma} (d^\dagger_{\mathbf{i},y,\sigma} d_{\mathbf{i}+\hat{x},y,\sigma} + d^\dagger_{\mathbf{i},x,\sigma} d_{\mathbf{i}+\hat{y},x,\sigma} + \mathrm{H.c.}) \\ & - t_3 \sum_{\mathbf{i},\sigma} (d^\dagger_{\mathbf{i},x,\sigma} d_{\mathbf{i}+\hat{x}+\hat{y},x,\sigma} + d^\dagger_{\mathbf{i},x,\sigma} d_{\mathbf{i}+\hat{x}-\hat{y},x,\sigma} \\ & + d^\dagger_{\mathbf{i},y,\sigma} d_{\mathbf{i}+\hat{x}+\hat{y},y,\sigma} + d^\dagger_{\mathbf{i},y,\sigma} d_{\mathbf{i}+\hat{x}-\hat{y},y,\sigma} + \mathrm{H.c.}) \\ & - t_4 \sum_{\mathbf{i},\sigma} (d^\dagger_{\mathbf{i},x,\sigma} d_{\mathbf{i}+\hat{x}+\hat{y},y,\sigma} + d^\dagger_{\mathbf{i},y,\sigma} d_{\mathbf{i}+\hat{x}+\hat{y},x,\sigma} + \mathrm{H.c.}) \\ & + t_4 \sum_{\mathbf{i},\sigma} (d^\dagger_{\mathbf{i},x,\sigma} d_{\mathbf{i}+\hat{x}-\hat{y},y,\sigma} + d^\dagger_{\mathbf{i},y,\sigma} d_{\mathbf{i}+\hat{x}-\hat{y},x,\sigma} + \mathrm{H.c.}), \end{aligned} \tag{1}$$

where $d^\dagger_{\mathbf{i},\alpha,\sigma}$ creates an electron with spin σ in the orbitals $\alpha = x, y$ (d_{xz} and d_{yz}, respectively) at site $\mathbf{i}$ of a 2D square lattice. $\hat{x}$ and $\hat{y}$ are unit vectors along the axes. The SK-evaluated Fe-Fe hopping amplitudes are $t_1 = -2[(b^2 - a^2) + g^2]/\Delta_{pd}$, $t_2 = -2[(b^2 - a^2) - g^2]/\Delta_{pd}$, $t_3 = -(a^2 + b^2 - g^2)/\Delta_{pd}$, and $t_4 = -(ab - g^2)/\Delta_{pd}$, where the Fe-As hopping amplitudes are $a = 0.324(pd\sigma) - 0.374(pd\pi)$, $b = 0.324(pd\sigma) + 0.123(pd\pi)$, and $g = 0.263(pd\sigma) + 0.31(pd\pi)$. $pd\sigma$ and $pd\pi$ are SK parameters and Δ_{pd} is the energy difference between the p and d levels. The overall energy scale is set by $(pd\sigma)^2/\Delta_{pd}$, which is of the order of eV and will be used as unit of energy. $pd\pi/pd\sigma$ is a free parameter in H_k. Equation (1) is formally the same as in Refs. [11,12], but the values for the hoppings are different: our approach relies on the analytic calculation of the hoppings in a "first-principles" SK-based context, while Ref. [11] fits the hoppings to bands from local-density approximation calculations. An interesting conclusion of our effort is that both sets of parameters lead to similar results for the magnetic order and the pairing. Equation (1) has invariance under the D_{4h} point-group [19], including a $\pi/2$ rotation of the lattice together with orbital exchanges $x \rightarrow y$ and $y \rightarrow -x$.

The on-site Coulombic terms include a Hubbard repulsion U for electrons with the same α, a repulsion U' for different α, a ferromagnetic Hund coupling J, and a pair-hopping term with strength $J' = J$ [20]:

$$\begin{aligned} H_{\mathrm{int}} = & U \sum_{\mathbf{i},\alpha} n_{\mathbf{i},\alpha,\uparrow} n_{\mathbf{i},\alpha,\downarrow} + (U' - J/2) \sum_{\mathbf{i}} n_{\mathbf{i},x} n_{\mathbf{i},y} \\ & - 2J \sum_{\mathbf{i}} \mathbf{S}_{\mathbf{i},x} \cdot \mathbf{S}_{\mathbf{i},y} \\ & + J \sum_{\mathbf{i}} (d^\dagger_{\mathbf{i},x,\uparrow} d^\dagger_{\mathbf{i},x,\downarrow} d_{\mathbf{i},y,\downarrow} d_{\mathbf{i},y,\uparrow} + \mathrm{H.c.}). \end{aligned} \tag{2}$$

$\mathbf{S}_{\mathbf{i},\alpha}$ ($n_{\mathbf{i},\alpha}$) is the spin (density) in orbital α at site $\mathbf{i}$. The standard relation $U' = U - 2J$ due to rotational invariance was used [21]. The full model becomes $H_{\mathrm{FeAs}} = H_k + H_{\mathrm{int}}$. Since the NN Fe-As-Fe bond angle θ_{NN} [Fig. 1(b)] is closer to 90° than the NNN Fe-As-Fe angle θ_{NNN} [Fig. 1(c)], we find a strong NNN hopping t_3 and the ratio t_3/t_1 is of order 1 for broad ranges of $pd\pi/pd\sigma$, without fine tuning. At intermediate to large U, the resulting effective Fe-Fe spin interaction along the plaquette diagonals consequently becomes as large as between NN Fe sites [14], or even larger. In the early days of HTSC, investigations of the resulting frustrated effective spin model unveiled a spin striped phase in the one-orbital model [22]. As shown in Figs. 1(d) and 1(e), the non-interacting system has electron FS around the (X, Y) points, and hole FS around the Γ and M points, which are equivalent on folding the Brillouin zone. 2-orbital models cannot have both hole pockets around the Γ point, as found in band structure calculations [8,9,11].

Magnetic properties in the undoped limit.—We study the ground state of model Eqs. (1) and (2) in the undoped limit by using two techniques: exact diagonalization (ED) and the variational cluster approach (VCA). The first method allows for an unbiased analysis, albeit restricted to small clusters [16], while the second extends the calculation to the bulk self-consistently [23,24]. We apply ED to the 2×2 and tilted $\sqrt{8} \times \sqrt{8}$ [Fig. 1(f)] clusters with periodic boundary conditions [16]. While the 2×2 cluster only has 4900 states even if no symmetries are used, the 8-sites cluster has 20 706 468 states with translational invariance

implemented, and is computationally demanding. We therefore fixed the ratio U/J to 4, compatible with some estimates [9]. However, other U/J ratios (to be discussed in future publications) do not critically affect the results presented below. In particular, the spin striped state and the singlet pairing (discussed later) survive for small J. The typical inequality $|pd\pi/pd\sigma| < 1$ is assumed, and the sign of $pd\pi$ is chosen such that the FS agrees with band structure calculations (see below). Both on the 2×2 and on the $\sqrt{8} \times \sqrt{8}$, we observe magnetic order with $q = (0, \pi), (\pi, 0)$ in real-space spin correlations as well as in the magnetic structure factor $S(q)$; see, e.g., Fig. 2(a). This leads us to believe that size effects are not severe. The $q = (0, \pi), (\pi, 0)$ state is stable at least in the large square $-0.5 < pd\pi/pd\sigma < 0$ and $0 < U < 4$, and it is generated by the robust plaquette-diagonal hoppings. We find similar results for both the SK hoppings and those of Ref. [11], and our results also agree with weak-coupling RPA approximations, where similar order arises from nesting [11,25]. Further evidence that we indeed identified the dominant magnetic channel comes from the VCA [23], where the self-energy of a small cluster is optimized by varying appropriate "fictitious" fields such as chemical potentials or symmetry-breaking staggered magnetic fields [23,24]. It thus combines the exact solution of a small cluster with access to the bulk limit [26]. The grand potential [Fig. 2(b)] demonstrates that the symmetry breaking indeed occurs in the $q = (0, \pi), (\pi, 0)$ channel. Figure 2(c) shows the stripe order parameter m_{stagg} (the staggered moment in units of Bohr magneton per Fe ion) vs U: we find a $(U, pd\pi/pd\sigma)$ regime that can accommodate the small m_{stagg} found with neutrons [5]. Note also that other experiments have reported larger m_{stagg} values [7].

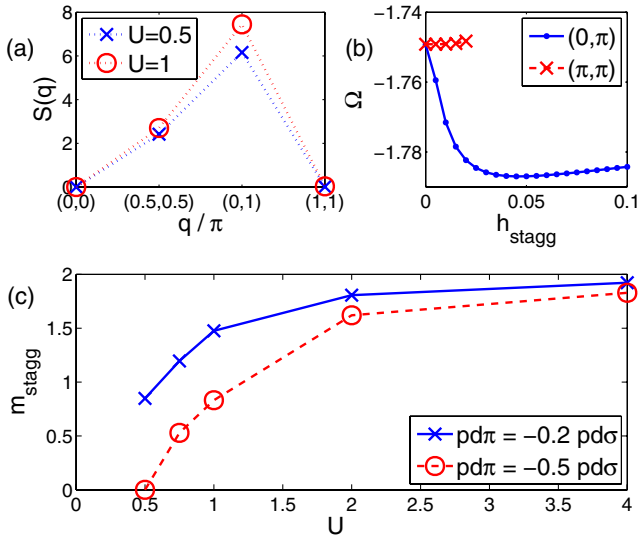

FIG. 2 (color online). (a) $S(q)$ vs q for the $\sqrt{8} \times \sqrt{8}$ cluster at the U's indicated, with $J = U/4$ and $pd\pi/pd\sigma = -0.2$. The momenta allowed in this cluster are (0, 0), ($\pm \pi/2, \pm\pi/2$), (0, π), (π, 0), and (π, π) [30]. (b) VCA grand potential [in energy units $(pd\sigma)^2/\Delta_{pd}$] vs staggered magnetic fields h_{stagg} for $\mathbf{q} = (\pi, \pi)$ and (0, π), and $pd\pi/pd\sigma = -0.2$, $U = 1$, $J = 0.25$, The minimum for (0, π) at $h_{\text{stagg}} \neq 0$ indicates symmetry breaking. (c) m_{stagg} vs U, with $U/J = 4$. The small U region at $pd\pi/pd\sigma = -0.2$ was numerically unstable.

Figure 3 shows photoemission spectra $A(\mathbf{k}, \omega)$. The first case (a) for $pd\pi/pd\sigma = -0.2$, $U = 0.5$ has a dispersion similar to that of the noninteracting system [Fig. 1(d)]; its FS is shown in Fig. 3(d) and the nodal structure will be discussed in a future publication. The density of states (DOS) has a small pseudogap [Fig. 3(c)], somewhat deeper than for $U = 0$, while larger $U = 2$ leads to an insulating hard gap. Another interesting regime is shown in (b): At $U = 1$ and $pd\pi/pd\sigma = -0.5$, the chemical potential lies in a region with many states, suggesting a correlated metal.

Pairing channels.—In the HTSC cuprates, the dominant pairing channel could be identified by adding two carriers to the undoped finite cluster (which has the same symmetries as the bulk system) and by then evaluating the quantum numbers under $\pi/2$ rotations [16]. Since NNN hoppings play a key role in the present case, we need at least a 2×2 cluster for *each sublattice*; the minimal cluster satisfying the requirement is the $\sqrt{8} \times \sqrt{8}$ cluster. Varying U and $pd\pi/pd\sigma$ ($U/J = 4$), we find that both singlet and triplet regimes can be reached by adding two electrons to the undoped (i.e., half-filled) system [27]; see the phase diagram in Fig. 4(a). At small $|pd\pi/pd\sigma|$ and intermediate or large U, the total spin is 0, and in searching for the local operator connecting the ground states of the

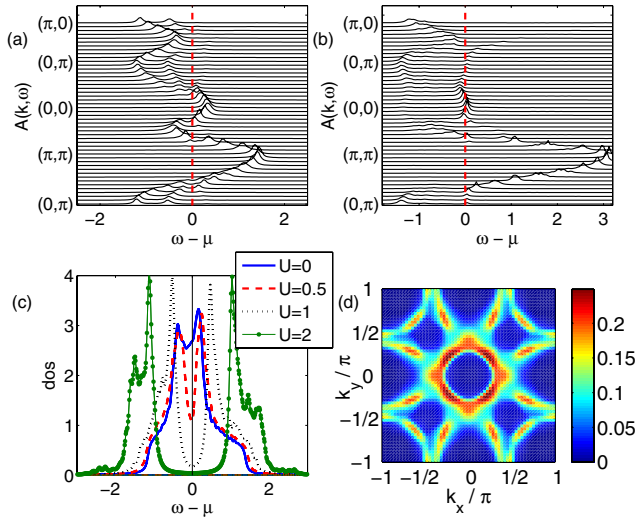

FIG. 3 (color online). One-particle VCA spectral function $A(\mathbf{k}, \omega)$ of H_{FeAs} for (a) $U = 0.5$, $J = 0.125$, and $pd\pi/pd\sigma = -0.2$, and (b) $U = 1$, $J = 0.25$, $pd\pi/pd\sigma = -0.5$ in the symmetry broken phase with (0, π) magnetic ordering at half-filling. A broadening 0.05 was used. (c) Density of states obtained by $\mathbf{k}$-integrating the spectral functions, at the U's indicated, with $U/J = 4$ and $pd\pi/pd\sigma = -0.2$. (d) FS corresponding to case (a). The FS has been symmetrized under rotations.

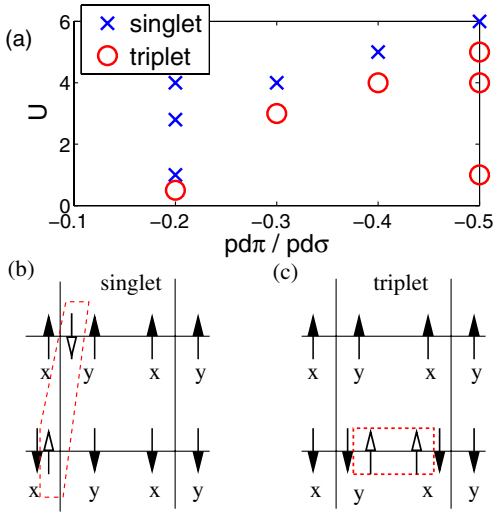

FIG. 4 (color online). (a) $\sqrt{8} \times \sqrt{8}$ cluster results with 2 more electrons than half-filling, at $U/J = 4$. Shown are regions with singlet and triplet pairing (see text). (b, c) Schematic representation of the singlet and triplet pairs (see text). Black arrows represent the magnetically ordered background. White arrows are the added electrons. x, y are the orbitals.

undoped and doped systems, the largest overlap at intermediate U is for

$$\Delta^\dagger(\mathbf{i}) = \sum_{\alpha,\hat{\mu}} (d^\dagger_{\mathbf{i},\alpha,\uparrow} d^\dagger_{\mathbf{i}+\hat{\mu},-\alpha,\downarrow} - d^\dagger_{\mathbf{i},\alpha,\downarrow} d^\dagger_{\mathbf{i}+\hat{\mu},-\alpha,\uparrow}), \qquad (3)$$

or in $\mathbf{k}$ space, $\Delta^\dagger(\mathbf{k}) = \sum_\alpha (\cos k_x + \cos k_y) d^\dagger_{\mathbf{k},\alpha,\uparrow} d^\dagger_{-\mathbf{k},-\alpha,\downarrow}$. $\alpha = x, y$ and $\hat{\mu} = \hat{x}, \hat{y}$. This operator is a spin singlet that transforms as the B_{2g} representation of the D_{4h} group [19], and it involves different x and y orbitals on NN sites to optimize the NN kinetic energy [Fig. 4(b)]. In other parts of the phase diagram, a spin-triplet dominates, which is odd under orbital exchange, transforms according to A_{2g} [19], and also involves different orbitals on NN sites [Fig. 4(c)]. Its projection-1 operator is

$$\Delta^\dagger(\mathbf{i})_1 = \sum_{\hat{\mu}} (d^\dagger_{\mathbf{i},x,\uparrow} d^\dagger_{\mathbf{i}+\hat{\mu},y,\uparrow} - d^\dagger_{\mathbf{i},y,\uparrow} d^\dagger_{\mathbf{i}+\hat{\mu},x,\uparrow}), \qquad (4)$$

that in momentum space becomes $\Delta^\dagger(\mathbf{k})_1 = (\cos k_x + \cos k_y)(d^\dagger_{\mathbf{k},x,\uparrow} d^\dagger_{-\mathbf{k},y,\uparrow} - d^\dagger_{\mathbf{k},y,\uparrow} d^\dagger_{-\mathbf{k},x,\uparrow})$. It resembles the operator of Ref. [15], although they use on-site pairing. Of the 16 possible pairing operators allowed by the symmetry of the Hamiltonian [19,28], our singlet and triplet operators correspond to No. 9 and No. 12 of Refs. [19,29].

Conclusions.—We studied a simple model for the FeAs superconductors numerically. The undoped system shows $q \sim (0, \pi), (\pi, 0)$ spin order. We identified dominant pairing operators for two added electrons: depending on parameters they can be spin singlet or triplet, transforming nontrivially under $\pi/2$ rotations. Future work will address more realistic models beyond two orbitals and contrast their results against those reported here.

We acknowledge discussions with F. Reboredo. Research supported by the NSF Grant No. DMR-0706020, the Div. of Materials Sciences and Eng., U.S. DOE under contract with UT-Batelle, LLC, and the Austrian Science Fund Grant No. P18551-N16.

[1] Y. Kamihara *et al.*, J. Am. Chem. Soc. **130**, 3296 (2008).
[2] Z.-A. Ren *et al.*, Chin. Phys. Lett. **25**, 2215 (2008); Europhys. Lett. **83**, 17 002 (2008).
[3] A. Sefat *et al.*, Phys. Rev. B **77**, 174503 (2008).
[4] L. Boeri *et al.*, Phys. Rev. Lett. **101**, 026403 (2008).
[5] C. de la Cruz *et al.*, Nature (London) **453**, 899 (2008).
[6] J. Dong *et al.*, Europhys. Lett. **83**, 27 006 (2008).
[7] A. I. Goldman *et al.*, Phys. Rev. B **78**, 100506 (2008); C. Krellner *et al.*, Phys. Rev. B **78**, 100504 (2008).
[8] D. J. Singh and M.-H. Du, Phys. Rev. Lett. **100**, 237003 (2008); G. Xu *et al.*, Europhys. Lett. **82**, 67 002 (2008).
[9] C. Cao *et al.*, Phys. Rev. B **77**, 220506 (2008).
[10] K. Haule *et al.*, Phys. Rev. Lett. **100**, 226402 (2008).
[11] S. Raghu *et al.*, Phys. Rev. B **77**, 220503 (2008).
[12] Q. Han *et al.*, Europhys. Lett. **82**, 37 007 (2008); T. Li, J. Phys. Condens. Matter **20**, 425203 (2008).
[13] K. Kuroki *et al.*, Phys. Rev. Lett. **101**, 087004 (2008); I. Mazin *et al.*, Phys. Rev. Lett. **101**, 057003 (2008); M. M. Korshunov and I. Eremin, Phys. Rev. B **78**, 140509(R) (2008); G. Baskaran, arXiv:0804.1341; P. Lee and X.-G. Wen, Phys. Rev. B **78**, 144517 (2008); Z.-J. Yao *et al.*, arXiv:0804.4166; X.-L. Qi *et al.*, arXiv:0804.4332.
[14] Q. Si and E. Abraham, Phys. Rev. Lett. **101**, 076401 (2008); C. Fang *et al.*, Phys. Rev. B **77**, 224509 (2008); C. Xu *et al.*, Phys. Rev. B **78**, 020501 (2008).
[15] X. Dai *et al.*, Phys. Rev. Lett. **101**, 057008 (2008); See also W. Chen *et al.*, arXiv:0808.3234.
[16] E. Dagotto, Rev. Mod. Phys. **66**, 763 (1994), and references therein.
[17] V. Vildosola *et al.*, Phys. Rev. B **78**, 064518 (2008).
[18] J. C. Slater and G. F. Koster, Phys. Rev. **94**, 1498 (1954).
[19] Y. Wan and Q.-H. Wang, arXiv:0805.0923.
[20] See e.g. A. M. Oles *et al.*, Phys. Rev. B **72**, 214431 (2005).
[21] Page 36 of E. Dagotto *et al.*, Phys. Rep. **344**, 1 (2001).
[22] C. Henley, Phys. Rev. Lett. **62**, 2056 (1989); E. Dagotto and A. Moreo, *ibid.* **63**, 2148 (1989).
[23] C. Dahnken *et al.*, Phys. Rev. B **70**, 245110 (2004).
[24] M. Potthoff, Eur. Phys. J. B **36**, 335 (2003).
[25] T. Yildirim, Phys. Rev. Lett. **101**, 057010 (2008).
[26] VCA is run on large but finite 48×48 lattices. We compared the $(0, \pi)$ phase to (π, π) and ferromagnetic order.
[27] As in "AF-broken-links" argumentations for HTSC [16], here pairing of carriers may emerge from the damage an added electron does to the magnetic background.
[28] Z.-H. Wang *et al.*, arXiv:0805.0736; Y. Zhou *et al.*, Phys. Rev. B **78**, 064514 (2008).
[29] In a future publication, we will show that similar results are also obtained using the parameters of Ref. [11].
[30] E. Dagotto *et al.*, Phys. Rev. B **41**, 9049 (1990).